ISSN 1063-7761, Journal of Experimental and Theoretical Physics, 2021, Vol. 133, No. 1, pp. 71–76. © Pleiades Publishing, Inc., 2021.
Russian Text © The Author(s), 2021, published in Zhurnal Eksperimental'noi i Teoreticheskoi Fiziki, 2021, Vol. 160, No. 1, pp. 88–94.

ORDER, DISORDER, AND PHASE TRANSITION IN CONDENSED SYSTEM

Realization Conditions and the Magnetic Field Dependence of Corner Excitations in the Topological Insulator with Superconducting Coupling on the Triangular Lattice

A. D. Fedoseev

Kirensky Institute of Physics, Federal Research Center KSC SB RAS, Krasnoyarsk, 660036 Russia
e-mail: fad@iph.krasn.ru

Received January 12, 2021; revised January 12, 2021; accepted February 13, 2021

Abstract—The studies of the topological properties of systems have recently been extended due to a new concept of higher-order topological insulators and superconductors. Many models were proposed for two-dimensional systems on a square lattice, where corner excitations can appear; however, the problem of existence of such excitations in superconducting systems with a triangular crystal lattice is still poorly understood. Using a topological insulator in the form of a triangle with a chiral superconducting order parameter as an example, we shows that corner excitations can exist in C_3-symmetric systems. In spite of a nontopological character, these excitations have energies inside the gap of the first-order edge excitation spectrum over a wide parameter range and are well localized at the corners of the system. Gapless corner excitations are shown to exist in the system at certain parameters. The application of a magnetic field in the system plane removes the triple degeneracy of the corner excitation energy and makes it possible to control the position of the minimum-energy corner excitation using a magnetic field. At the same time the fine adjustment to achieve the gapless excitations at the chosen corner can be made with changing of the magnetic field value.

DOI: 10.1134/S1063776121060029

INTRODUCTION

The studies of topologically nontrivial systems have recently received a new direction related to the concept of higher-order topological insulators (HOTIs) [1]. In such systems, both the spectrum of bulk states and the spectrum of first-order edge states are gapped, and edge states appear at higher-order boundaries, namely, corners in two-dimensional systems and corners and hinges in three-dimensional systems, appear. It should be noted that, before [1], the authors of [2, 3] demonstrated the possibility of appearance of localized states at domain walls between regions with different topological indices located at an open system boundary.

Higher-order topological systems are of particular interest due to the possibility of appearance of Majorana corner states in two-dimensional higher-order topological superconductors (HOTSCs) [4, 5], since they solve one of the problems of creating Majorana states in practice. First-order Majorana states require a purely one-dimensional system, which can hardly be achieved in practice, and the broadening of a chain gives rise to the appearance of a gapless edge excitation band. Although zero-energy excitations are still separated from bulk excitations in this case, they are not separated from other edge excitations. In addition, when a one-dimensional system broadens, the character of excitations changes from a purely Majorana character to a chiral one, which is accompanied by a change in the length-to-width ratio of the system [6, 7]. The predicted Majorana corner states solve these problems. First, their energy lies in the gap of the spectra of both bulk and edge excitations. Second, their localization exactly at system corners hinders a change in the character, and they are still Majorana states irrespective of the length-to-width ratio of the system.

Additional interest in HOTSC is caused by the possibility of changing the position of corner excitations by varying the system parameters [5, 8, 9]. The corner excitations in two-dimensional systems are thought to be good candidates for braiding, which is one of the key requirements for creating a topological qubit [10]. Another possible practical application of such systems is the possibility of creating nanodevices with controlled transport characteristics on their basis. For such practical applications to be implemented, it is important to control corner excitations using external fields, which was demonstrated in [5, 8].

The widely used approach used to create HOTSC consists in considering a topological insulator model with allowance for superconducting coupling chosen so that the spectrum of first-order edge excitations acquires a gap and the Dirac mass for these excitations has opposite signs at contacting boundaries [4]. In this

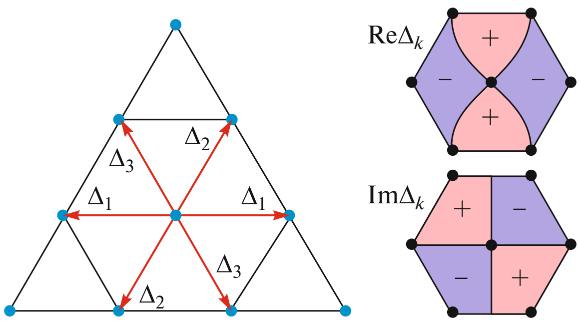

Fig. 1. Chiral superconducting pairing of the $d + id$ type on the triangular lattice. (on the left) Direction of superconducting pairing Δ_j (Eq. (2)). (on the right) Signs of $\mathrm{Re}\Delta_k$ and $\mathrm{Im}\Delta_k$ [29]. (points) Nodal points Δ_k (Eq. (3)).

case, the corners in a system serve as domain walls at which second-order edge excitations would appear, i.e., as gapless corner excitations. This approach works well in systems on a square crystal lattice, for which numerous HOTI and HOTSC models were proposed [11–15]. However, this approach cannot be applied to C_3-symmetric systems, since an even number of topologically protected corner states always appear in terms of the method described above [16].

Another method for forming corner states was suggested using the Kagome lattice as an example [17–19]. At certain parameters, the sites located at the corners of a system with open boundary conditions in the form of a triangle become isolated from the remaining system to form corner states (similarly to the edge states in the Su–Schrieffer–Heeger model or the Kitaev model [20]). These states are gapless and appear in the entire parameter region, which is not separated from a specific parametric point by closing the gap in an edge state spectrum. The authors of [18, 19] suppose that such states are topologically protected by generalized chiral symmetry. However, the key feature of the systems under study was the absence of electron–hole symmetry; therefore, such an approach cannot be applied to create HOTSC. Moreover, the conclusions about the topological protection of corner states in the Kagome lattice were disputed later [21, 22]. In addition, the authors of [21] concluded that topologically protected corner states cannot exist in a C_3-symmetric system.

Although the topologically protected corner states in systems in the form of a triangle, which have a triangular crystal lattice, are prohibited, these systems are still of interest. First, there exist other manifestations of the nontrivial topology apart from the appearance of gapless corner states [16]. In particular, a charge anomaly can appear in a C_3-symmetric system [23]. Second, edge states, including gapless ones, can appear in the systems that do not provide their topological protection. For example, edge states were detected in the trivial phase of a one-dimensional chain with spin–orbit coupling and s-type superconductivity [24, 25] and an exciton insulator with a spin–orbit coupling [26]. Zero-energy edge excitations were found in the trivial phase of a two-dimensional topological insulator with chiral superconductivity and 120-degree magnetic ordering [27, 28].

Since systems with a triangular lattice do not have topologically protected corner states, it is important to study the possibility of existence of nontopological corner excitations, including gapless corner excitations, in such a system. The purpose of this work is to study the conditions of appearance of corner excitations in a two-dimensional topological insulator in the form of a triangle with chiral superconductivity on a triangular lattice and their modification in an applied magnetic field.

MODEL FOR TOPOLOGICAL INSULATOR WITH CHIRAL SUPERCONDUCTIVITY ON THE TRIANGULAR LATTICE

Similarly to [4], we consider a two-level model in the tight-binding approximation and take into account the hybridization induced by the Rashba spin–orbit coupling and the superconducting singlet pairing at neighboring sites,

$$\begin{aligned}
\hat{H} &= \hat{H}_0 + \hat{T} + \hat{H}_{so} + \hat{H}_{sc},\\
\hat{H}_0 &= \sum_{f\nu\sigma} (\nu\Delta\varepsilon - \mu) c^{\dagger}_{f\nu\sigma} c_{f\nu\sigma},\\
\hat{T} &= t \sum_{\langle fm\rangle\nu\sigma} \nu c^{\dagger}_{f\nu\sigma} c_{m\nu\sigma},\\
\hat{H}_{so} &= i\lambda \sum_{\langle fm\rangle\nu\sigma\sigma'} [\boldsymbol{\sigma}_{\sigma\sigma'} \times \mathbf{d}_{fm}]_z c^{\dagger}_{f\nu\sigma} c_{m,-\nu,\sigma'},\\
\hat{H}_{sc} &= \sum_{\langle fm\rangle\nu} \Delta_{fm} c^{\dagger}_{f\nu\uparrow} c^{\dagger}_{m\nu\downarrow} + \text{h.c.}
\end{aligned} \tag{1}$$

Here, the sum over f means summation over lattice sites, $\langle fm\rangle$ corresponds to summation over the nearest neighbors, $\mathbf{d}_{fm}$ is the unit vector along the direction from site m to site f, μ is the chemical potential of the system, $2\Delta\varepsilon$ is the difference between the site energies in two subbands, t is the parameter of hopping between the nearest neighbors, λ is the spin–orbit coupling parameter, σ_j are the Pauli matrices in the spin space, and $c^{\dagger}_{f\nu\sigma}$ are the operators of electron creation at site f in different subbands designated by index $\nu = \pm 1$.

We consider the case of chiral superconducting singlet pairing between electrons at the nearest sites corresponding to the symmetry of a triangular lattice (Fig. 1),

$$\Delta_{fm} = \Delta_j = \Delta_1 e^{2\pi i (j-1)/3}, \quad j = 1, 2, 3. \tag{2}$$

The bulk excitation spectrum of the system has the form

$$E_k = \sqrt{|\Delta_k|^2 + (\mu - E_k^{TI})^2}. \quad (3)$$

Here, E_k^{TI} is the bulk excitation spectrum in a topological insulator,

$$\begin{aligned} E_k^{TI} &= \pm\sqrt{|t_k|^2 + |\lambda_{k\sigma}|^2}, \\ t_k &= \Delta\varepsilon - 2t + 4t\cos\frac{k_x}{2}\left(\cos\frac{k_x}{2} + \cos\frac{k_y\sqrt{3}}{2}\right), \\ \lambda_{k\sigma} &= 2i\lambda\sigma\sin\frac{k_x}{2}\left(2\cos\frac{k_x}{2} + \cos\frac{k_y\sqrt{3}}{2}\right) \\ &\quad -2\sqrt{3}\lambda\sin\frac{k_y\sqrt{3}}{2}\cos\frac{k_x}{2}, \end{aligned} \quad (4)$$

Δ_k is the superconducting pairing, which has the two-dimensional representation

$$\begin{aligned} \Delta_k &= 2\Delta_1\left(\cos k_x - \cos\frac{k_x}{2}\cos\frac{k_y\sqrt{3}}{2}\right) \\ &\quad -2i\sqrt{3}\Delta_1\sin\frac{k_x}{2}\sin\frac{k_y\sqrt{3}}{2}. \end{aligned} \quad (5)$$

Since Δ_k has two-dimensional representation, it has nodal points, as spin–orbit coupling, rather than nodal lines, as in [4].

In the absence of superconducting pairing, Hamiltonian (1) describes a two-dimensional chiral topological insulator characterized by the Chern spin number [30]

$$\begin{aligned} C_s &= 1, \quad -6t < \Delta\varepsilon < 2t, \\ C_s &= 2, \quad 2t < \Delta\varepsilon < 3t. \end{aligned} \quad (6)$$

In the absence of hybridization between subbands, the investigated system is a topological superconductor [31, 32] with opposite Chern numbers in the upper and lower subbands,

$$C_\nu = 2\nu, \quad -3t + \Delta\varepsilon < \nu\mu < 6t + \Delta\varepsilon. \quad (7)$$

It should be noted that, since the Chern numbers have opposite signs, the total Chern number of the system at the intersection of nontrivial regions for the upper and lower subbands is $C = 0$. Therefore, the system is sensitive to hybridization between subbands.

When chiral superconducting pairing and spin–orbit coupling are taken into account simultaneously, the diagram of topological phases remains the same as in the absence of spin–orbit coupling. The trivial regions with $C_{\pm 1} = 0$ remain trivial, and the regions where only one of the Chern numbers is $C_{\pm 1} \neq 0$ and the other is $C_{\mp 1} = 0$ remain topologically nontrivial. Both regions are not interesting for searching corner excitations. The region in which both Chern numbers $C_{\pm 1}$ are nonzero forms a topological phase with Chern number $C = 0$, which now has no topologically protected edge excitations. However, both nontopological edge excitations, including gapless ones, and corner excitations can exist within this region. Therefore, we will study this region below.

CORNER EXCITATIONS IN A TRIANGULAR SYSTEM

The results of numerical calculation of the single-electron excitations of a topological triangular insulator with chiral superconductivity demonstrate the presence of three situations in the region under study depending on the parameters (Fig. 2, on the left). First-order gapless edge excitations appear in the system in a significant part of the region despite the fact that it is topologically trivial. The second part of the region corresponds to nontopological corner excitations with energy inside the gap in the edge excitation spectrum. The energy of such excitations is triply degenerate because of the equivalence of the corners in the system. The third case corresponds to the presence of a gap in the system in the spectrum of first-order edge excitations, and corner excitations with an energy inside the gap are absent in the system.

A mutual correspondence between the energy and character of edge excitations exists in one-dimensional systems. If the energy of a state is inside the gap of a bulk spectrum, the state is an edge one; if the energy of a state inside the spectrum of allowed bulk states, the state is a bulk one. This correspondence in two-dimensional systems is valid only in one direction. If the energy of a state is inside the absolute gap of a bulk state spectrum, this state is still an edge one. However, the converse is generally speaking wrong. The same is true of the corner excitations in two-dimensional systems. Therefore, to determine the character of states in two-dimensional cases, it is useful to calculate the inverse participation ratio (IPR) [33, 34], which characterizes the localization of a state. This parameter approved itself for detecting edge states in topological insulators [35],

$$I_q(m) = \frac{\sum_f (A_m(f))^q}{\left(\sum_f A_m(f)\right)^q}, \quad (8)$$

where $A_m(f)$ is the amplitude of excitation with number m at site f and $q > 1$. Parameter I_q is relatively high for localized states ($I_q = 1$ for a state localized at one site) and has an order of $1/V^{q-1}$ for a delocalized state in a system with V sites.

Figure 3 shows I_4 as a function of chemical potential μ for various eigenexcitations in the system. The excitations characterized by the minimum energy at $\mu = 0$ are seen to remain well localized at triangle corners even when the energy is outside the gap of the edge excitation spectrum in the system (Fig. 3d). Small I_4 peaks appear due to the tendency of first-

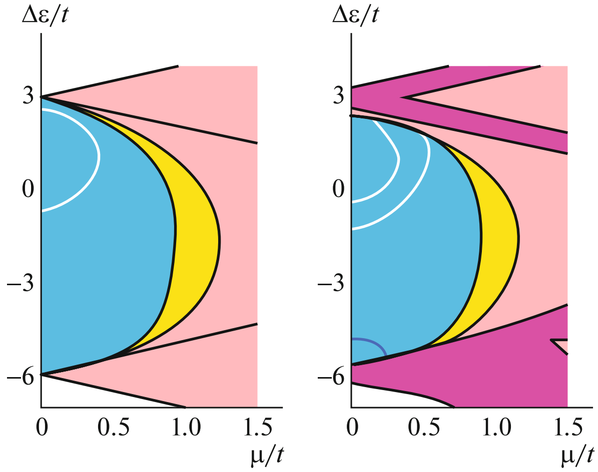

Fig. 2. Parameter diagram of a topological triangular insulator with chiral superconductivity on a triangular lattice. (on the left) In the absence of magnetic field; (on the right) in the presence of in-plane magnetic field at $h = 0.3$ and $\phi_h = \pi/2$. Red regions correspond to first-order gapless edge excitations, and violet regions correspond to gapless bulk excitations. Blue regions correspond to the parameter regions in which corner excitations with energies inside the edge excitation spectrum gap appear in the system. In yellow parameter regions, an edge excitation spectrum has a gap and corner excitations with energies inside the gap are absent. The white line corresponds to the parameters at which gapless corner excitations appear, and the blue line corresponds to the parameters at which the edge excitation spectrum gap closes in a magnetic field. The spin–orbit coupling parameter is $\lambda = 0.5t$, and the superconducting pairing parameter is $\Delta_1/t = 0.5$.

order edge excitations with energies deep in the gap of the bulk excitation spectrum toward localization at the corners of limited systems [36]. Such excitations can easily be distinguished from corner excitations by changing the system size. Since edge excitations are distributed over the entire system boundary even in the presence of the tendency toward localization at the corners, their IPR values decrease with increasing system size. In contrast, the IPR values of the corner states remain unchanged.

Zero-energy corner excitations can appear in the system at certain values of the parameters forming a line in the parameter diagram (Fig. 2, on the left). These zero-mode lines do not represent the size effect, in contrast to the situations considered in [25, 37, 38]. The presence of a disorder in the system does not affect the possibility of existence of zero-energy corner excitations in it. However, the values of the parameters at which such excitations appear turned out to be very sensitive to the disorder at the corners of the system.

EFFECT OF MAGNETIC FIELD ON THE REALIZATION CONDITIONS OF CORNER EXCITATIONS

We now consider the influence of a homogeneous magnetic field directed in the system plane on the cor-

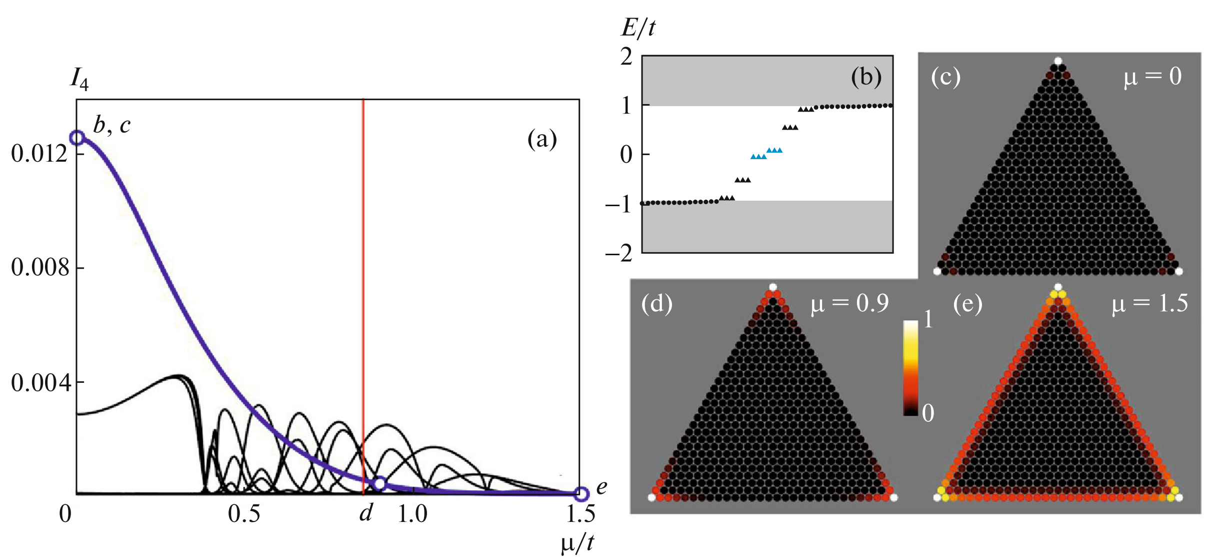

Fig. 3. (a) I_4 (Eq. (8)) of the eigenexcitations in a triangular topological insulator with chiral superconductivity vs. chemical potential. (blue line) Corner excitations with the minimum energy and (red line) chemical potential μ at which the corner excitation energy intersects the boundary of the edge excitation region. (b) Spectrum of the system at $\mu = 0$: (points) edge excitation energies, (triangles) corner excitation energies, (gray regions) edge state band. (c–e) Spatial distribution of corner excitations at various chemical potentials designated by points in (a): at $\mu = 0$, the corner excitation with an energy inside the edge excitation spectrum gap; at $\mu = 0.9t$, the corner excitation with an energy inside the edge state band; at $\mu = 1.5t$, the excitation is an edge one and tends toward localization at system corners. The system parameters are as follows: $\Delta_1/t = 0.6$, $\Delta\varepsilon = 0$, and $\lambda/t = 0.5$.

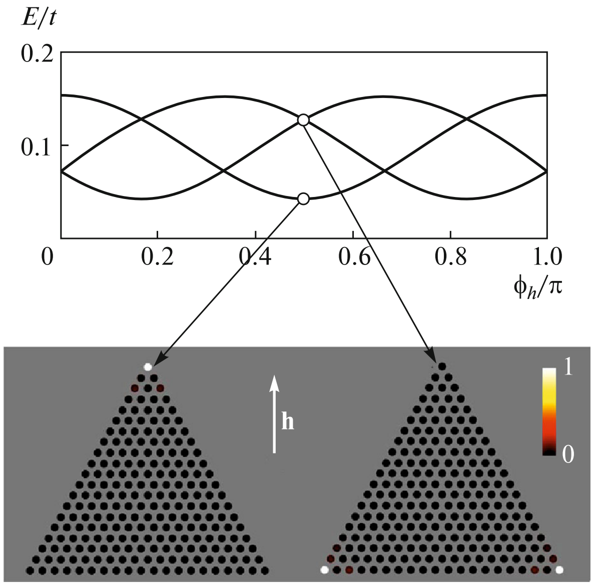

Fig. 4. (top) Corner excitation energy vs. the direction of magnetic field $h = 0.3t$ directed in the system plane. (bottom) Spatial distribution of two minimum-energy excitations at $\phi_h = \pi/2$.

ner states in a triangular topological insulator with chiral superconductivity on a triangular lattice,

$$\hat{H}_h = -\sum_{f\nu\sigma\sigma'} \mathbf{h}\boldsymbol{\sigma}_{\sigma\sigma'} c^{\dagger}_{f\nu\sigma} c_{f\nu\sigma'},$$
$$\mathbf{h} = h(\cos\phi_h, \sin\phi_h, 0). \tag{9}$$

An applied magnetic field changes the parameter diagram described in the previous section (Fig. 2, on the right). For example, the bulk excitation spectrum closes in the parameter region rather than at lines. In addition, a parameter line, which corresponds to the closing of the gap in the first-order edge excitation spectrum, appears inside the parameter region corresponding to corner excitations. When a magnetic field is applied, the line of gapless corner modes splits into two lines. However, the regions of corner excitations remain almost the same.

Since the spin and space degrees of freedom are interrelated in the investigated system due to spin–orbit coupling, the application of a magnetic field in the system plane breaks the spatial symmetry and makes the corners nonequivalent. In this case, the excitation energy depends on both the magnitude and direction of magnetic field (Fig. 4). For example, the excitation located at the angle the direction to which from the center of the triangle coincides with magnetic field direction has an extremum energy. Thus, using a magnetic field, we can finely adjust the system to form a zero-energy corner excitation and determine the angle at which this excitation appears.

Since the excitations induced by a magnetic field have a nontopological character and cannot be represented in the form of two split Majorana operators, this system cannot be used for braiding. However, it can be useful for a device, the transport through which can be controlled by a magnetic field.

CONCLUSIONS

Using a two-dimensional triangular topological insulator with chiral superconductivity on the triangular lattice, we demonstrated the possibility of existence of corner excitations in C_3-symmetric systems. The corner excitations in such a system were shown to have energies both inside and outside the gap of a first-order edge excitation spectrum. The corner excitations are gapless at certain values of the parameters that form a line in the parameter diagram. The application of a magnetic field to the system removes the degeneracy of corner excitations, and the corner excitation energy depends on both the magnitude of a magnetic field and its direction in the system plane. This finding makes it possible to perform fine adjustment to achieve zero-energy corner excitation and to choose the angle at which this excitation exists.

ACKNOWLEDGMENTS

I thank D.M. Dzebisashvili, V.A. Mitskan, M.S. Shustin, M.M. Korovushkin, and S.V. Aksenov for numerous helpful discussions and attention to the work.

FUNDING

This work was supported by the Russian Foundation for Basic Research (project no. 19-02-00348), Government of Krasnoyarsk Territory, Krasnoyarsk Regional Fund of Science to the research projects: "Study of edge states in one- and two-dimensional topological superconductors" (no. 20-42-243005), "Coulomb interactions in the problem of Majorana modes in low-dimensional systems with nontrivial topology" (no. 19-42-240011), and Council of the President of the Russian Federation for Support of Young Scientists and Leading Scientific Schools (Project MK-1641.2020.2).

REFERENCES

1. W. A. Benalcazar, B. A. Bernevig, and T. L. Hughes, Science (Washington, DC, U. S.) **357**, 61 (2017).
2. G. E. Volovik, JETP Lett. **91**, 201 (2010).
3. F. Zhang, C. L. Kane, and E. J. Mele, Phys. Rev. Lett. **110**, 046404 (2013).
4. Q. Wang, C.-C. Liu, Yu.-M. Lu, and F. Zhang, Phys. Rev. Lett. **121**, 186801 (2018).
5. X. Zhu, Phys. Rev. B **97**, 205134 (2018).
6. A. C. Potter and P. A. Lee, Phys. Rev. Lett. **105**, 227003 (2010).
7. N. Sedlmayr, J. M. Aguiar-Hualde, and C. Bena, Phys. Rev. B **93**, 155425 (2016).

8. T. E. Pahomi, M. Sigrist, and A. A. Sluyanov, Phys. Rev. Res. **2**, 032068(R) (2020).
9. S.-B. Zhang, A. Calzona, and B. Trauzettel, Phys. Rev. B **102**, 100503(R) (2020).
10. C. Nayak, S. H. Simon, A. Stern, M. Freedman, and S. D. Sarma, Rev. Mod. Phys. **80**, 1083 (2008).
11. A. Yoshida, Y. Otaki, R. Otaki, and T. Fukui, Phys. Rev. B **100**, 125125 (2019).
12. J. Zou, Zh. He, and G. Xu, Phys. Rev. B **100**, 235137 (2019).
13. Q.-B. Zeng, Y.-B. Yang, and Y. Xu, Phys. Rev. B **101**, 241104(R) (2020).
14. K. Asaga and T. Fukui, Phys. Rev. B **102**, 115102 (2020).
15. S.-B. Zhang, W. B. Rui, A. Calzona, S.-J. Choi, A. P. Schnyder, and B. Trauzettel, Phys. Rev. Res. **2**, 043025 (2020).
16. E. Khalaf, W. A. Benalcazar, T. L. Hughes, and R. Queiroz, arXiv: 1908.00011 (2019).
17. M. Ezawa, Phys. Rev. Lett. **120**, 026801 (2018).
18. X. Ni, M. Weiner, A. Alu, and B. Khanikaev, Nat. Mater. **18**, 113 (2019).
19. S. N. Kempkes, M. R. Slot, J. J. van den Broeke, P. Capoid, W. A. Benalcazar, D. Vanmaekelbergh, D. Cercioux, I. Swart, and C. M. Smith, Nat. Mater. **18**, 1292 (2019).
20. A. Yu. Kitaev, Phys. Usp. **44** (Suppl.), 131 (2001).
21. G. van Miert and C. Ortix, Quantum Mater. **5**, 63 (2020).
22. M. Jung, Y. Yu, and G. Shvets, arXiv: 2010.10299 (2020).
23. W. A. Benalcazar, T. Li, and T. L. Hughes, Phys. Rev. B **99**, 245151 (2019).
24. M. Serina, D. Loss, and J. Klinovaja, Phys. Rev. B **98**, 035419 (2018).
25. A. D. Fedoseev, J. Exp. Theor. Phys. **128**, 125 (2019).
26. V. V. Val'kov, JETP Lett. **111**, 647 (2020).
27. V. V. Val'kov, A. O. Zlotnikov, A. D. Fedoseev, and M. S. Shustin, J. Magn. Magn. Mater. **440**, 37 (2017).
28. V. V. Val'kov, A. O. Zlotnikov, and M. S. Shustin, J. Magn. Magn. Mater. **459**, 112 (2018).
29. A. M. Black-Schaffer and C. Honerkamp, J. Phys.: Condens. Matter **26**, 423201 (2014).
30. M. Ezawa, Eur. Phys. J. B **85**, 363 (2012).
31. T. Senthil, J. B. Marston, and M. P. A. Fisher, Phys. Rev. B **60**, 4245 (1999).
32. T. Chern, AIP Adv. **6**, 085211 (2016).
33. D. J. Thouless, Phys. Rep. **13**, 93 (1974).
34. N. C. Murphy, R. Wortis, and W. A. Atkinson, Phys. Rev. B **83**, 184206 (2011).
35. M. Calixto and E. Romera, J. Stat. Mech. **2015**, 06029 (2015).
36. A. D. Fedoseev, J. Phys.: Condens. Matter **32**, 215301 (2020).
37. V. V. Val'kov, V. A. Mitskan, and M. S. Shustin, JETP Lett. **106**, 798 (2017).
38. V. V. Val'kov, V. A. Mitskan, and M. S. Shustin, J. Exp. Theor. Phys. **129**, 426 (2019).

Translated by K. Shakhlevich